NASA TECHNICAL NOTE

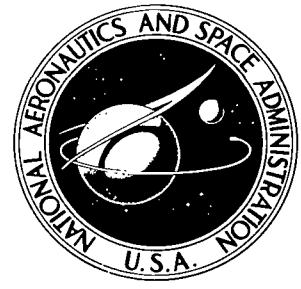

NASA TN D-6547

DEVELOPMENT AND INITIAL OPERATING CHARACTERISTICS OF THE 20-MEGAWATT LINEAR PLASMA ACCELERATOR FACILITY

by Arlen F. Carter, Willard R. Weaver, Donald R. McFarland, and George P. Wood

Langley Research Center
Hampton, Va. 23365

NATIONAL AERONAUTICS AND SPACE ADMINISTRATION • WASHINGTON, D. C. • DECEMBER 1971

1. Report No.	2. Government Accession No.	3. Recipient's Catalog No.
NASA TN D-6547		

4. Title and Subtitle
DEVELOPMENT AND INITIAL OPERATING CHARACTERISTICS OF THE 20-MEGAWATT LINEAR PLASMA ACCELERATOR FACILITY

5. Report Date
December 1971

6. Performing Organization Code

7. Author(s)
Arlen F. Carter, Willard R. Weaver, Donald R. McFarland, and George P. Wood

8. Performing Organization Report No.
L-7932

10. Work Unit No.
112-02-22-01

9. Performing Organization Name and Address
NASA Langley Research Center
Hampton, Va. 23365

11. Contract or Grant No.

13. Type of Report and Period Covered
Technical Note

12. Sponsoring Agency Name and Address
National Aeronautics and Space Administration
Washington, D.C. 20546

14. Sponsoring Agency Code

15. Supplementary Notes

16. Abstract

The 20-megawatt linear plasma accelerator facility at the Langley Research Center, which is a steady-flow, Faraday-type plasma accelerator facility for high-velocity aerodynamic testing, has been constructed, developed, and brought to an operational status. The accelerator has a 63.5-mm-square and 0.5-meter-long channel and utilizes nitrogen seeded with 2-percent mole fraction of cesium vapor. Modification of the original accelerator design characteristics and the improvements necessary to make the arc heater a suitable plasma source are described. The measured accelerator electrode current distribution and the electrode-wall potential distributions are given; the computed and the measured values are in good agreement. Measured pitot pressure indicates that an accelerator exit velocity of 9.2 km/sec, which is 81 percent of the computed velocity of 11.3 km/sec, is obtained with 30 of the 36 electrode pairs powered and corresponds to a velocity increase to about $2\frac{1}{4}$ times the computed entrance velocity. The computed stagnation enthalpy at the accelerator exit is 92 MJ/kg, an increase of 71 MJ/kg from the entrance value of 21 MJ/kg, and the mass density corresponds to an altitude of about 58 km. The 92 MJ/kg stagnation enthalpy corresponds to a kinetic-energy content at low temperature equivalent to a velocity of 13.6 km/sec. This accelerator appears to be the largest and highest velocity nonpulsed linear plasma accelerator to attain an operable status.

17. Key Words (Suggested by Author(s))	18. Distribution Statement
Magnetohydrodynamics High-enthalpy, high-density flow Faraday accelerator Plasma accelerator Arc heater	Unclassified – Unlimited

19. Security Classif. (of this report)	20. Security Classif. (of this page)	21. No. of Pages	22. Price*
Unclassified	Unclassified	33	$3.00

*For sale by the National Technical Information Service, Springfield, Virginia 22151

DEVELOPMENT AND INITIAL OPERATING CHARACTERISTICS OF THE 20-MEGAWATT LINEAR PLASMA ACCELERATOR FACILITY

By Arlen F. Carter, Willard R. Weaver, Donald R. McFarland, and George P. Wood
Langley Research Center

SUMMARY

The program to develop a linear, steady-flow, Faraday-type plasma accelerator facility has culminated in the successful operation of the 20-megawatt linear plasma accelerator facility at the Langley Research Center. The design of the facility was based on the theoretical models developed and the experimental findings obtained from earlier work with smaller channel sizes. The accelerator channel is 63.5 mm square and 0.5 meter long, the electrode walls are segmented into 36 electrode pairs, and the duration of a test is 3 seconds with longer test times possible.

The following modifications to the original design necessary to make the facility operational are presented and discussed: (1) the arc-heater cathode was replaced by a multiple cathode that operates with negligible erosion; (2) the magnetic field of the arc-heater anode was changed to eliminate destructive arcing between the anode and adjacent sections of the arc heater; (3) the accelerator magnet pole pieces were modified and the magnet was operated in an over-design condition to obtain the desired distribution of magnetic-flux density; (4) the mass-flow rate was reduced by a factor of two to allow operation of the arc heater at the original design enthalpy level; (5) the accelerator current density was reduced by a factor of two to avoid erosion of the accelerator electrodes and the insulators and to maintain the Hall potential gradient at the original design value; (6) the destructive arcing between the accelerator and the test section was eliminated.

Although flow-diagnostic measurements are limited, observation of the flow about a pitot tube indicates (1) the flow is supersonic and (2) the accelerator significantly increases the flow Mach number. Measured pitot pressure indicates an exit velocity of 9.2 km/sec, which is 81 percent of the computed velocity of 11.3 km/sec, with 30 of the 36 electrode pairs powered. This value corresponds to a velocity increase to about $2\frac{1}{4}$ times the computed entrance velocity. The computed stagnation enthalpy is increased from 21 MJ/kg at the accelerator entrance to 92 MJ/kg at the accelerator exit, which corresponds to a kinetic-energy content at low temperature equivalent to a velocity of 13.6 km/sec, and the mass density corresponds to an altitude of about 58 km. The data indicate that the facility is operable near the computed conditions. This accelerator appears to be the largest and highest velocity nonpulsed linear plasma accelerator to attain an operable status.

INTRODUCTION

The Langley Research Center has been engaged in a program to develop a linear, steady-flow, Faraday-type plasma accelerator facility for high-velocity aerodynamic testing. Initial theoretical and design ground work for the program was laid in reference 1. References 2 and 3 reported the first successful experiments in the steady-state acceleration of plasma with a linear, dc, cross-field accelerator at a moderately high density. References 4 to 8 contain further refinements to the theoretical description of plasma acceleration and experimental results obtained with channel sizes up to 25.4 mm by 25.4 mm in cross section.

Based on the theoretical models developed and the experimental findings obtained from this earlier work, an accelerator facility was designed that would produce a higher speed flow (approximately 13 km/sec), would have a larger channel cross-sectional area (63.5 mm by 63.5 mm), and would be more suitable for diagnostics and aerodynamic testing. The original design details of this facility, the 20-megawatt linear plasma accelerator facility at the Langley Research Center, are reported in reference 9. The facility has been constructed, developed, and brought to an operational status (ref. 10) with 30 of the 36 accelerator electrode pairs powered.

The present paper reports some of the experiences and problems encountered in developing and making operational this facility. The paper compares some of the operating parameters with the computed parameters of the facility.

SYMBOLS

a	speed of sound, m/sec
B	magnetic-flux density, teslas
c_p	specific heat at constant pressure, J/kg-K
c_v	specific heat at constant volume, J/kg-K
e	elementary charge, coulombs
E	electric-field strength, V/m
f	friction factor, dimensionless
j	current density, A/m^2

M	Mach number, u/a
n	number density, $meter^{-3}$
p	pressure, N/m^2
$p_{t,2}$	pitot pressure, N/m^2
T	temperature, kelvins
u	velocity, m/sec
V	potential difference, volts
x	distance in axial (flow) direction, meters
y	distance in direction of applied electric field of accelerator, meters
z	distance in direction of magnetic field of accelerator, meters
γ	ratio of specific heats, $\frac{c_p}{c_v}$
ρ	mass density, kg/m^3
τ	mean free time, seconds
ω	cyclotron frequency, $second^{-1}$

Subscripts:

e	electron
x	component in x-direction
y	component in y-direction
z	component in z-direction

GENERAL DESCRIPTION OF FACILITY

A schematic diagram of the 20-MW accelerator facility, which is a linear, steady-flow, Faraday-type plasma accelerator facility, is shown in figure 1. The arc-heater plasma source consists of a cathode, constrictor, transition section, anode, and plenum chamber. The working gas is nitrogen seeded with 2-percent mole fraction (based on molecular nitrogen) of cesium vapor, which is injected into the flow at the plenum chamber. Immediately downstream of the plenum chamber is the supersonic nozzle, which is followed by the accelerator. The nozzle exit conditions, listed in table I, are used as the accelerator entrance conditions. One 10-MW power supply is used to power the arc heater, and a second 10-MW power supply is used for the accelerator. The accelerator channel is 63.5 mm square and 0.5 meter long and the electrode walls are segmented into 36 electrode pairs. Immediately downstream of the accelerator is a test section used for observation and diagnostics of the flow. The test section is followed by an exhaust duct cooled by water sprayed on its outer surface. A steam-ejector pumping system provides a vacuum source. Figure 2 shows part of the facility; the upstream end of the accelerator is exposed and the accelerator cooling-water hoses and electrical leads are disconnected. A more complete description of the facility components and their design details is given in reference 9.

MODIFICATION OF ARC-HEATER CATHODE

The original arc-heater cathode did not satisfactorily meet the original design specifications; consequently, the cathode was modified to improve its performance. The cathode was designed to operate at approximately 3 kA in a nitrogen atmosphere at a pressure of about 200 kN/m^2. The design lifetime was 5 hours, but in operation the cathode eroded until unusable in approximately 20 minutes. The excessive cathode-erosion rate necessitated frequent replacement of the arc attachment surface of the cathode assembly and frequent cleaning of the interior surfaces of the arc heater that were being coated by material eroded from the cathode.

The original cathode is shown in detail in figure 3. It consists of a brass cylinder body that is water cooled. A 12.7-mm-diameter passage at the center of the cathode is used for injection of part of the working gas. The discharge is rotated about the flow axis on the arc attachment surface of the cathode by the magnetic field of a water-cooled coil embedded within the cathode and immediately behind the cathode face. At first the arc attachment surface was made of oxygen-free hard copper, but its resistance to erosion was very poor. A tungsten-base refractory alloy (75 percent tungsten and 25 percent copper by weight) was substituted for the copper, gave improved erosion resistance, and extended the lifetime of the cathode to about 1 hour. Although improved, the cathode-

erosion rate and lifetime were unsatisfactory. Frequent cleaning of the interior surfaces of the arc heater coated by the material eroded from the cathode and frequent replacement of the arc attachment surface were still necessary. Furthermore, the refractory alloy was inferior in that it developed radial cracks, probably because of thermal stress, that permitted water to leak through the arc attachment surface. The rather short lifetime of the cathode prompted a search for a better cathode material and/or a different geometry to improve the lifetime.

The design of arc-heater cathodes suitable to handle several megawatts of power has very little theoretical basis. Most of the cathodes in present use were developed by long-term testing programs, and no one type or geometry has emerged as being clearly superior. The type preferred by many investigators for use in nitrogen is the "button type" cathode that consists of a tungsten or tungsten-alloy disk embedded in a water-cooled copper base. According to Charles E. Shepard of the NASA Ames Research Center, a 2-percent-thoriated tungsten button has been used at a stagnation pressure of 100 kN/m^2 in nitrogen to carry as much as 3 kA with little erosion. This limit, however, was too close to the continuous-operation point of the arc heater, and the use of this type of cathode was considered to be too nearly marginal.

Reference 11 reports tests to determine the current-carrying capacity of thermionic-emitting cathodes in a nitrogen atmosphere. A cathode with a conical tip similar to the one of figure 4 was used for most tests. Three types of tungsten were used: thoriated, barium-oxided, and barium-calcium-aluminated. The cathode of barium-calcium-aluminated tungsten was markedly superior in the current range of 100 to 500 amperes; at a pressure of 100 kN/m^2, a 12.7-mm-diameter cathode could operate at 500 amperes with no noticeable erosion. A suitable electrode might be one with a multiple-cathode geometry with as many individual current-carrying elements as was necessary to handle the 3-kA requirement. This approach is similar to that of reference 12 which reported the grouping of three cathodes at much lower arc-power levels.

The success of a multiple-cathode arrangement depends on whether or not the current can be suitably divided among individual cathode elements. One approach is to use a small (less than 1 ohm) series resistance with each cathode element to cause an element with increased or decreased current to drop or to rise to a different potential than the other elements. The current should then shift until all elements carry the same amount of current and reach the same potential. Tests were conducted with a cathode constructed of six of the 12.7-mm-diameter cathode elements shown in figure 4 equally spaced on a 31.8-mm-diameter circle and mounted axially within the arc heater, as shown in figure 5. A series resistance of 0.1 ohm with each element was found to be sufficient to distribute the current uniformly within about 10 percent. However, with this configuration the arc would not remain on the conical tips; it tended to locate at the inside surfaces of the

elements at the intersection of the cone and the cylindrical body. The resultant asymmetrical heating of the tip produced serious thermal cracking of the barium-calcium-aluminated tungsten tip; large pieces of tip material broke off from the cathode elements. (The barium-calcium-aluminated tungsten was later discovered to be degraded by atmospheric moisture. Unless carefully protected, the original material would break up and crumble when left undisturbed on the shelf. Since the material used in the electrode tests was always new and protected from atmospheric moisture, its degradation is not considered to be a factor in the electrode cracking.) The nitrogen working gas had been injected downstream of the elements, and in an attempt to move the arc attachment point back toward the tip, part of the gas was injected axially through the center of the cathode cluster. This adjustment resulted in some alleviation of the problem but not enough for the performance to be acceptable.

The geometry of the electrode cluster therefore was changed to that shown in figure 6. Each element is the same as that shown in figure 4, but the six elements are distributed in a radial configuration perpendicular to the flow axis. The nitrogen gas flow was injected downstream of the cathode elements so that they operated in somewhat of a stilled atmosphere. With this geometry, the arc attachment remained on the conical tips and each element carried 500 amperes with no noticeable erosion and, consequently, negligible coating of the surfaces in the constrictor section and other parts of the arc heater.

Initially, some thermal cracking of the tips took place with the radial configuration, but this cracking was eliminated by shortening the distance between the tip of an element and the cooling water to approximately 9.5 mm and by changing the cone apex angle from 90° to 120°.

Some difficulty also has been experienced with the constrictor wall at the point that the multiple cathode elements extend into the constrictor. In the vicinity of the cathodes the constrictor wall is a cylindrical copper sleeve (51 mm in diameter) which extends 76 mm upstream and 56 mm downstream of the multiple cathode. The arc current has a tendency to be short-circuited by the downstream part of the constrictor wall rather than to be conducted through the gas. Although the constrictor wall is highly cooled by water, it was not designed to support a sustained discharge of several thousand amperes, and severe local heating and considerable erosion occur at the discharge. The constrictor wall is being modified so that it is segmented in the same manner as the rest of the constrictor. (See ref. 9.) The segmentation of the wall should break up the discharge path and prevent further difficulties.

MODIFICATION OF ANODE MAGNETIC FIELD

The anode of the arc heater was designed with an external coil, placed in series with the anode power lead, that generates a magnetic field to rotate the anode spot to prevent excessive erosion or burnout of the electrode. The coil produced a distribution of axial magnetic-flux density at the surface of the anode, as indicated in figure 7. The maximum flux density occurred at the center of the anode, and the arc preferred to be attached in the weaker field at either end of the anode. The anode spot most often attached itself near the downstream edge of the anode, and considerable arcing occurred between the anode and the plenum section immediately downstream. Sporadic arcing also occurred upstream of the anode between the anode and the transition section that joins the constrictor to the anode. Neither the transition section nor the plenum was designed to carry large currents, and the arcing caused local melting. The arc was also attaching much nearer the point of cesium injection than was desirable. Therefore, modification of the distribution of anode magnetic-flux density was necessary.

The distribution was changed so that the anode spot would be confined to the central part of the anode. To accomplish this change, the axial component of the field was made large near the upstream and the downstream ends of the anode to prevent the discharge from coming to the wall in these regions and was reduced in the central region of the anode to allow the discharge to come to the wall near the center of the anode. The desired distribution of magnetic-flux density was obtained by considering the layered coil windings to be a current sheet. Reference 13 gives data for the magnetic-flux density produced by a semi-infinite current sheet. The computed fields from any number of current sheets for various coils may be algebraically added to obtain the resultant distribution.

In this manner the desired distribution of magnetic-flux density was obtained and is given in figure 8. The maximum flux density is approximately 0.3 tesla and occurs just downstream of the anode. At the middle of the anode, the flux density is reduced to approximately 0.07 tesla, which is the minimum value at the anode with the original coil and a value that is satisfactory in preventing anode erosion and burnout. The flux density reaches another peak at the upstream end of the anode at a value of approximately 0.16 tesla. At this location the flux density at the arc-heater center line is approximately 0.03 tesla less than that at the electrode wall; this lower flux density is helpful in keeping the discharge away from the wall. The measured distribution of flux density was found to vary less than 15 percent from the computed values.

The coils used to produce the modified flux-density distribution are also shown in figure 8. The three coils are mounted close to the outer surface of the anode: one coil of 30 turns is located at the downstream end of the anode, a second coil of eight turns is located near the middle of the anode and is wound in a reverse direction to partially cancel

the field of the first coil; a third coil of four turns is located near the upstream end of the anode and is wound in the same direction as the first coil. The coils are made of square copper tubing, 9.5 mm by 9.5 mm, with a 6.9-mm-diameter cooling passage; the copper tube is wrapped in fiber glass for electrical insulation, and the coil is coated with epoxy for strength and rigidity. The coils are in series with each other and with the anode electrical power lead and are cooled by the high-pressure water system of the arc heater.

Modification of the anode-flux-density distribution has entirely eliminated the arcing between the anode and the adjacent components; the arc heater operates smoothly with this distribution, and the anode spot appears to be attaching to the wall near the center of the anode.

ARC-HEATER OPERATION WITH CESIUM SEEDING

A major concern in the original design of the 20-MW accelerator facility was the effect of the fringing magnetic field of the accelerator magnet on the operation of the arc heater and the supersonic nozzle with cesium-seeded flow. As described in reference 9, the magnetic-flux density of the accelerator magnet was necessarily large in the region of the arc-heater anode, plenum, and supersonic nozzle. The anode and the plenum are upstream of the nozzle, and the anode spot is made to rotate by a solenoidal magnetic field to prevent burnout of the anode. If the flux density from the accelerator magnet was strong in this region, the discharge might not rotate properly and might burn out or severely erode the anode. The nozzle wall is constructed from a solid piece of copper; therefore, any currents induced in the plasma by its motion through a magnetic field are short-circuited both across the nozzle at right angles to the flow and in the axial direction. This short circuiting could reduce the flow velocity, change the velocity or pressure distribution, and if the currents are large enough, possibly increase the nozzle-wall temperature to the point of failure.

To avoid these difficulties with the arc-heater and supersonic-nozzle system, the flux density of the accelerator magnet was reduced from its original design value. It was uncertain, however, that this reduction was sufficient to avoid possible difficulty.

Before the effect of the magnetic field of the accelerator magnet on the arc-heater and supersonic-nozzle system could be determined, the arc heater had to be operated with cesium seeding and without the accelerator magnetic field since past experience had indicated that the seeding itself was also a potential source of trouble. (See refs. 6 and 7.) The seeding system described in reference 9 was used with a cesium mass-flow rate of 1.8 g/sec (2-percent mole fraction based on molecular nitrogen) to inject cesium vapor into the arc-heater flow. No significant effect on the arc-heater operating characteristics resulted; the observed flow from the nozzle was smooth and appeared to be uniform.

Apparently, the cesium vapor was uniformly dispersed in the nitrogen plasma and was not finding its way upstream into the region of the anode.

To determine the effect of the accelerator magnet on the operation with cesium seeding of the arc-heater and supersonic-nozzle system, a water-cooled cylindrical channel was attached to the nozzle exit as a substitute for the accelerator, and the magnet was installed in its proper relation to the arc heater and supersonic nozzle. The magnet was energized at a very low current level, and the arc heater was turned on. With the flow unseeded, the magnet current was increased to its operating value; no change in arc-heater operating characteristics was observed. The procedure was repeated with the flow seeded; the result was the same; that is, no instability of the arc heater was observed nor was there any significant change in operational characteristics, the nozzle was not noticeably affected, and no measurable increase in energy dissipation to the nozzle walls was noted. Therefore, the compromise made in the distribution of the flux density of the accelerator magnet reported in reference 9 to maintain a low value of flux density in the vicinity of the nozzle and the anode of the arc heater was acceptable inasmuch as no unsatisfactory operation of the arc-heater and supersonic-nozzle system was experienced.

MODIFICATION OF ACCELERATOR DESIGN PARAMETERS

Initial tests of the arc heater indicated that the original design enthalpy of 23 MJ/kg could not be obtained at the desired mass-flow rate of 36.3 g/sec. The failure of the arc heater to meet the original design specification made modification of the accelerator facility necessary because the design of this facility had been accomplished with the assumption of a specific set of accelerator entrance conditions. Any significant reduction in arc-heater enthalpy would change the accelerator entrance conditions, especially the velocity, and invalidate the accelerator design.

At this point in the development of the facility, certain aspects of the original design, for example, the length and the cross-sectional area of the accelerator channel, the number of accelerator electrode pairs, and the accelerator magnet design, had been fixed and could not be easily and economically changed. With the configuration of the accelerator and the magnet fixed and the entrance velocity of the accelerator reduced because of the inadequate performance of the arc heater, the only way to attain the desired accelerator exit velocity was to increase the current density in the accelerator. The attainment of an exit velocity of 12.9 km/sec was important; it was one of the major goals of the accelerator design. An increase in current density, however, would increase the likelihood of erosion of the accelerator electrodes and insulators. The original design current density at the first electrode was 360 kA/m^2. This current density is approximately twice the current density that was successfully used in the 1-inch-square plasma accelerator at the Langley Research Center. The high current density together with the fact that the current

concentrates at the leading edge of the cathodes and the trailing edge of the anodes indicated that no increase in current density should be considered. In fact, further consideration of the possibility of severe electrode and insulator erosion over the upstream part of the channel due to the original design current density indicated that a reduction, rather than an increase, in the current density was desirable.

The most reasonable way, therefore, to correct for the arc-heater enthalpy deficiency was to reduce the mass-flow rate from the original design value of 36.3 g/sec to 18.2 g/sec. At this mass-flow rate, the arc heater was capable of producing an enthalpy close to the original design value. The value of accelerator current density was also decreased by a factor of two. This decrease was made for two reasons: (1) the current density would be equal to or below the value used successfully in the 1-inch-square plasma accelerator, and (2) the Hall potential gradient would remain unchanged from the original design value. The assumption was made that the Hall potential gradient

$$E_x = \frac{j_y B_z}{n_e e}$$

would remain constant because the decrease in j_y would be offset by the decrease in n_e. Maintaining E_x at the original design value was important because, as stated in reference 9, from the microscopic point of view the accelerating force derives principally from the ions. The ions, moving essentially in the direction of the channel axis and accelerating the neutrals, derive their energy from the Hall potential field. From this point of view, if the original design exit velocity is to be obtained, the design value of E_x must be maintained.

A change in the distribution of the accelerator magnetic flux density also was necessary when the magnet, powered at the 400-ampere design value, produced a flux density significantly different from the original design value. Figure 9 shows the discrepancy between the original design and the measured flux densities. The discrepancy was largely overcome because the design flexibility incorporated in the magnet allowed operation at a higher current and permitted changes in the pole pieces. The magnet could be operated at up to 600 amperes without causing significant overheating of the coil windings. Slight modifications to the pole pieces were made and operation at 600 amperes gave a flux-density distribution that was sufficiently close to the original design value to be acceptable. (See fig. 9.)

Because of the changes in accelerator current density, mass-flow rate, magnetic-flux density, and arc-heater operating characteristics, computation of a new set of accelerator operating parameters was necessary. The inlet conditions for the accelerator (see table I) were those values computed as the nozzle exit conditions based on the measured stagnation conditions of the arc heater (stagnation pressure, 105 kN/m^2; stagnation enthalpy, 20.9 MJ/kg). The coefficient of viscosity of nitrogen was calculated from

reference 14 to be 0.1 g/m-sec. By use of the methods of reference 9, the friction factor f was calculated to be 0.017 ($\omega_e \tau_e$ was estimated from ref. 15 to be approximately 30), and the effective electrical conductivity was calculated to be 150 mhos/m.

The above revised parameters were incorporated in the numerical integration of the equations describing accelerator performance that are given in reference 9. The velocity distribution is given in figure 10 and is seen to reach 12.1 km/sec at an accelerator length of about 0.48 meter. In figures 10 through 16, accelerator parameters are given from the first electrode (x = 0.034 meter) to the thirty-sixth electrode (x = 0.478 meter) with the accelerator channel entrance taken to be at an axial distance x = 0. The computed distributions of current density, applied electrode potential difference, static pressure, static temperature, mass density, and Mach number are given in figures 11 through 16, respectively.

The modifications in the accelerator design necessary to make the facility operational have resulted in a computed exit velocity of 12.1 km/sec at a mass density that corresponds to an altitude of 58 km. This velocity compares very favorably with the exit velocity of 12.9 km/sec at a mass density that corresponds to an altitude of 53 km, which was the original design goal for the facility (ref. 9).

OPERATING CHARACTERISTICS OF ACCELERATOR

A major part of the development, since the accelerator was first powered, has centered around the matching of the voltage required by the accelerator to the voltage available from the 10-MW power supply. A schematic diagram of the resistor network and the connections to the power supply is shown in figure 17. A full description of the details of this part of the facility is contained in reference 9. The matching of the voltage required by the accelerator to the voltage available from the existing power supply was accomplished by operating the accelerator with only the upstream one-third of the electrode pairs energized and adjusting the resistors in both the anode and the cathode circuits to obtain the desired electrode current level and the proper match between the axial component of the applied potential distribution and the internally generated Hall potential distribution so that axial currents were reduced to very low values. After the resistors for the first one-third of the 36 electrode pairs were properly adjusted by this procedure, additional electrode pairs were added, and at present, the resistors have been adjusted for the first 30 of the 36 electrode pairs. The remaining electrode pairs are not powered in order to avoid erosion damage to the downstream endplate of the accelerator. (See ref. 9 for details of accelerator construction.) The duration of a typical test is 3 seconds with longer test times possible.

The measured electrode current distribution is shown in figure 18. The upstream currents of 120 to 140 amperes correspond to current densities of 150 to 175 kA/m^2, whereas the downstream currents of about 80 to 90 amperes are approximately constant and correspond to current densities of 100 to 110 kA/m^2. The experimental values closely match the computed values shown in figure 18 as the solid line. The measured axial, or Hall, current is typically 10 percent or less of the current through a pair of electrodes, and if the currents are considered to be uniformly distributed throughout the channel, the ratio of transverse current density to Hall current density is approximately 50 to 1. Figure 19 gives the measured and computed distribution of anode- and cathode-wall potentials. The computed Hall potential gradient is approximately 35 volts per electrode, and when combined with the computed difference of applied electrode potential, the resultant anode-wall and cathode-wall potential gradients along most of the channel length are 2740 V/m and 2880 V/m, respectively. The measured anode-wall and cathode-wall potential gradients along most of the channel length are 3160 V/m and 2720 V/m, respectively, and are in reasonably good agreement with the computed values.

During initial tests, arcing to the grounded test section on the cathode side of the channel was noted. Little melting of the test section occurred with only one-third of the electrodes powered, but as more electrodes were added, the arcing became progressively more destructive. Careful examination of the interior of the test section showed evidence of minor arcing to edges of window openings, corners, and some flat surfaces. Motion-picture films confirmed the presence of arcing from the flow to the interior walls of the test section. It was apparent that some of the current from the anodes was going downstream and attaching to the interior of the test section, then returning upstream, perhaps through the boundary layers, from the cathode side of the test section to the various cathodes. From the amount of material loss and melting, the current was estimated to be on the order of hundreds of amperes. Limited measurements made with a Rogowski coil at the accelerator exit confirmed that the current was in excess of 500 amperes.

To prevent the destructive arcing, the interior of the stainless-steel test section was arc sprayed with a 0.51-mm-thick coating of aluminum oxide, boron nitride insulators were installed at the exit of the accelerator to provide a longer breakdown path for the discharge, and all openings around windows and access ports were sealed with nonpriming silicon rubber (the nonpriming type acts as a gasket and is easily removed). The destructive arcing was eliminated by these procedures; however, slight, very minor, arcing still occurs at the edges of the windows where the silicon rubber seal does not, at times, seal the opening completely.

DIAGNOSTICS OF FLOW AT ACCELERATOR EXIT

At present, only limited diagnostic data have been obtained of the flow at the accelerator exit. However, the flow at the accelerator exit is supersonic. With the accelerator unpowered, the flow exhibits a distinct shock-wave pattern at the accelerator exit. When a pitot tube is inserted into the flow, a bow shock wave can be seen. The shock-wave standoff distance is approximately 5.9 mm, or 0.41 of the radius of the pitot tube. The shock wave away from the vicinity of the pitot tube is too indistinct for obtaining a good measure of the shock-wave angle.

Figure 20 shows the flow about a pitot tube with the accelerator powered; the bow shock is well defined. The shock-wave standoff distance is about 2.4 mm, or 0.17 of the radius of the pitot tube, and the shock-wave angle (measured from the upstream-flow direction) is about 40°. The large decrease in shock-wave standoff distance when the accelerator is powered indicates a significant increase in the flow Mach number by the accelerator.

The measured pitot pressure at the accelerator exit is usually one of the simpler flow-diagnostic tests to make; however, in high-enthalpy, high-density flow such as that produced by the accelerator, this normally simple measurement is greatly complicated by the extreme heating rate to which the probe is subjected. A pitot tube that is highly cooled by high-pressure (10 MN/m^2) water was designed and built. It was successfully used in the high-enthalpy flow at a stagnation-point heat-transfer rate (calculated on the basis of a body diameter of 25.4 mm) of 52 MW/m^2 to measure a pitot pressure of 45 kN/m^2 at the accelerator exit on the flow center line. The measured pitot pressure with the accelerator unpowered was 10.3 kN/m^2. The significant increase in pitot pressure obtained with the accelerator powered is an important qualitative indicator of accelerator performance since the Lorentz force increases the stagnation pressure of the flow, whether the flow is supersonic or subsonic, whereas the joule heating decreases the stagnation pressure in either velocity range.

The pitot pressure is generally expressed in terms of Mach number and the ratio of specific heats γ; both are quantities that are not known to a good degree of accuracy in high-velocity plasma flows. If, however, the ratio of pitot pressure to ρu^2 given by

$$\frac{p_{t,2}}{\rho u^2} = \frac{1}{\gamma M^2}\left[\frac{(\gamma + 1)M^2}{2}\right]^{\frac{\gamma}{\gamma-1}}\left[\frac{\gamma + 1}{2\gamma M^2 - (\gamma - 1)}\right]^{\frac{1}{\gamma-1}}$$

is considered, the ratio is found to be approximately equal to unity over a wide range of Mach number and γ. Figure 21 indicates the variation of the ratio of pitot pressure to ρu^2 as a function of Mach number for values of γ of 1.1 and 1.4. Above a Mach number

of 2.5, the ratio of pitot pressure to ρu^2 is unity with a maximum uncertainty of about 8 percent for any value of γ between 1.1 and 1.4. The pitot pressure, therefore, is a good measure of ρu^2, and if the assumption is made that the known value of ρu is uniformly distributed throughout the channel, the velocity can be obtained from the measured pitot pressure without exact knowledge of other gas parameters.

If the measured pitot pressure with the accelerator powered is combined with the mass flow per unit channel area of 4.56 kg/m^2-sec (the total mass-flow rate, including cesium-seeded material, is 19.9 g/sec), the velocity is calculated to be 9.2 km/sec. This velocity is 81 percent of the computed velocity of 11.3 km/sec for the 30 powered electrode pairs. This agreement is a good indication that the accelerator is operating near the computed conditions. The velocity, based on the measured pitot pressure, corresponds to a velocity increase to about $2\frac{1}{4}$ times the computed entrance velocity, and the stagnation enthalpy is increased from 21 MJ/kg to an estimated 92 MJ/kg. This latter value corresponds to a kinetic-energy content at low temperature equivalent to a velocity of 13.6 km/sec.

CONCLUDING REMARKS

The 20-megawatt linear plasma accelerator facility at the Langley Research Center, which is a steady-flow, Faraday-type plasma accelerator facility for high-velocity aerodynamic testing, has been constructed, developed, and brought to an operational status. The following modifications to the original design necessary to make the facility operational were accomplished: (1) the arc-heater cathode was replaced by a multiple cathode that operates with negligible erosion; (2) the magnetic field of the arc-heater anode was changed to eliminate destructive arcing between the anode and adjacent sections of the arc heater; (3) the accelerator magnet pole pieces were modified and the magnet operated in an over-design condition to obtain the desired distribution of magnetic-flux density; (4) the mass-flow rate was reduced by a factor of two to allow operation of the arc heater at the original design enthalpy level; (5) the accelerator current density was reduced by a factor of two to avoid erosion of the accelerator electrodes and the insulators and to maintain the Hall potential gradient at the original design value; (6) the destructive arcing between the accelerator and the test section was eliminated.

Successful operation of the arc heater and supersonic nozzle was achieved without adverse effects from either injection of cesium vapor into the plenum or operation of the accelerator magnet at the desired flux density. The accelerator resistor network was successfully adjusted to obtain the desired accelerator current distribution and to match the axial component of the applied potential distribution to the internally generated Hall potential distribution.

The accelerator was operated with 30 of the 36 electrode pairs powered, and the measured accelerator electrical parameters agreed well with the computed values: The current-density distribution was successfully adjusted to match the computed values, the ratio of transverse current density to Hall current density was about 50 to 1, and the Hall potential gradient was measured and found to be only about 10 percent different from the computed value.

A pitot tube highly cooled by deionized water was constructed and successfully operated in the high-enthalpy flow at a calculated stagnation-point heating rate of 52 MW/m^2. Although flow-diagnostic measurements are limited, the flow from the accelerator exit was found to be supersonic from observation of the bow shock wave on the pitot tube; the significant change observed in the shock-wave angle and the shock-wave standoff distance indicated that when powered the accelerator significantly increased the flow Mach number. Measured pitot pressure indicated an exit velocity of 9.2 km/sec, which is 81 percent of the computed velocity of 11.3 km/sec, with 30 of 36 electrode pairs powered. This value corresponds to a velocity increase to about $2\frac{1}{4}$ times the computed entrance velocity. The computed stagnation enthalpy is increased from 21 MJ/kg at the accelerator entrance to 92 MJ/kg at the accelerator exit, which corresponds to a kinetic-energy content at low temperature equivalent to a velocity of 13.6 km/sec, and the mass density corresponds to an altitude of about 58 km. The data indicate that the facility is operable near the computed conditions. The accelerator appears to be the largest and highest velocity nonpulsed linear plasma accelerator to attain an operable status.

Langley Research Center,
National Aeronautics and Space Administration,
Hampton, Va., October 29, 1971.

REFERENCES

1. Wood, George P.; and Carter, Arlen F.: Considerations in the Design of a Steady DC Plasma Accelerator. Dynamics of Conducting Gases, Ali Bulent Cambel and John B. Fenn, eds., Northwestern Univ. Press, c.1960, pp. 201-212.

2. Wood, George P.: Analysis of Steady-Flow Plasma Accelerator. Bull. Amer. Phys. Soc., ser. II, vol. 6, no. 2, Mar. 20, 1961, pp. 187-188.

3. Wood, George P.; Carter, Arlen F.; Sabol, Alexander P.; and Weinstein, Richard H.: Experiments in Steady State Crossed-Field Acceleration of Plasma. Phys. Fluids, vol. 4, no. 5, May 1961, pp. 652-653.

4. Wood, George P.; Carter, Arlen F.; Lintz, Hubert K.; and Pennington, J. Byron: A Theoretical Treatment of the Steady-Flow, Linear, Crossed-Field, Direct-Current Plasma Accelerator for Inviscid, Adiabatic, Isothermal, Constant-Area Flow. NASA TR R-114, 1961.

5. Carter, Arlen F.; Wood, George P.; Sabol, Alexander P.; and Weinstein, Richard H.: Experiments in Steady-State High-Density Plasma Acceleration. Engineering Aspects of Magnetohydrodynamics, Clifford Mannal and Norman W. Mather, eds., Columbia Univ. Press, 1962, pp. 45-55.

6. Wood, G. P.; Carter, A. F.; Sabol, A. P.; McFarland, D. R.; and Weaver, W. R.: Research on Linear Crossed-Field Steady-Flow d.c. Plasma Accelerators at Langley Research Center, NASA. Arc Heaters and MHD Accelerators for Aerodynamic Purposes, Pt. I, AGARDograph 84, Sept. 1964, pp. 1-45.

7. Carter, A. F.; Wood, G. P.; McFarland, D. R.; and Weaver, W. R.: Research on a Linear Direct-Current Plasma Accelerator. AIAA J., vol. 3, no. 6, June 1965, pp. 1040-1045.

8. Carter, A. F.; McFarland, D. R.; Weaver, W. R.; Park, S. K.; and Wood, G. P.: Operating Characteristics, Velocity and Pitot Distribution, and Material Evaluation Tests in the Langley One-Inch-Square Plasma Accelerator. AIAA Paper No. 66-180, Am. Inst. Aeron. Astronaut., Mar. 1966.

9. Carter, Arlen F.; Weaver, Willard R.; McFarland, Donald R.; Park, Stephen K.; and Wood, George P.: Design of the 20-Megawatt Linear Plasma Accelerator Facility. NASA TN D-6115, 1971.

10. Weaver, W. R.; McFarland, D. R.; Carter, A. F.; and Wood, G. P.: Design and Operational Characteristics of the Langley 20-Megawatt Plasma Accelerator Facility. 11th Symposium on Engineering Aspects of Magnetohydrodynamics, California Inst. Technol., Mar. 1970, pp. 77-81.

11. Anon.: Experiments to Establish Current-Carrying Capacity of Thermionic-Emitting Cathodes. AVSSD-0043-67-RR (Contract No. NAS2-3379), AVCO Corp., Jan. 30, 1967. (Available as NASA CR-73186.)

12. Boldman, Donald R.; Shepard, Charles E.; and Fakan, John C.: Electrode Configurations for a Wind-Tunnel Heater Incorporating the Magnetically Spun Electric Arc. NASA TN D-1222, 1962.

13. Alexander, Nancy B; and Downing, Arthur C.: Tables for a Semi-Infinite Circular Current Sheet. ORNL-2828, U.S. At. Energy Comm., Oct. 13, 1959.

14. Ahtye, Warren F.; and Peng, Tzy-Cheng: Approximations for the Thermodynamic and Transport Properties of High-Temperature Nitrogen With Shock-Tube Applications. NASA TN D-1303, 1962.

15. Weber, R. E.; and Tempelmeyer, K. E.: Calculation of the D-C Electrical Conductivity of Equilibrium Nitrogen and Argon Plasma With and Without Alkali Metal Seed. AEDC-TR-64-119, U.S. Air Force, July 1964.

TABLE I.- COMPUTED CONDITIONS FOR THE 20-MEGAWATT LINEAR PLASMA ACCELERATOR FACILITY AT THE LANGLEY RESEARCH CENTER

[Based on 30 of 36 electrode pairs powered]

Condition	At accelerator entrance (a)	At accelerator exit
Velocity, km/sec	4.13	11.3
Density, g/m^3	1.17	[b] 0.414
Temperature, kK	5.2	5.8
Pressure, kN/m^2	1.96	1.08
Enthalpy (stagnation), MJ/kg	20.9	91.7
Mach number	3.0	6.6
Mass-flow rate (nitrogen), g/sec	18.2	18.2
Channel cross-sectional width, mm	63.5	63.5
Channel cross-sectional height, mm	63.5	63.5
Reynolds number per meter	---	46 000
Stagnation-point heat-transfer rate (based on body diameter of 25.4 mm), MW/m^2	---	52.0

[a] Same as nozzle-exit conditions.

[b] Equivalent to an altitude of 58 km.

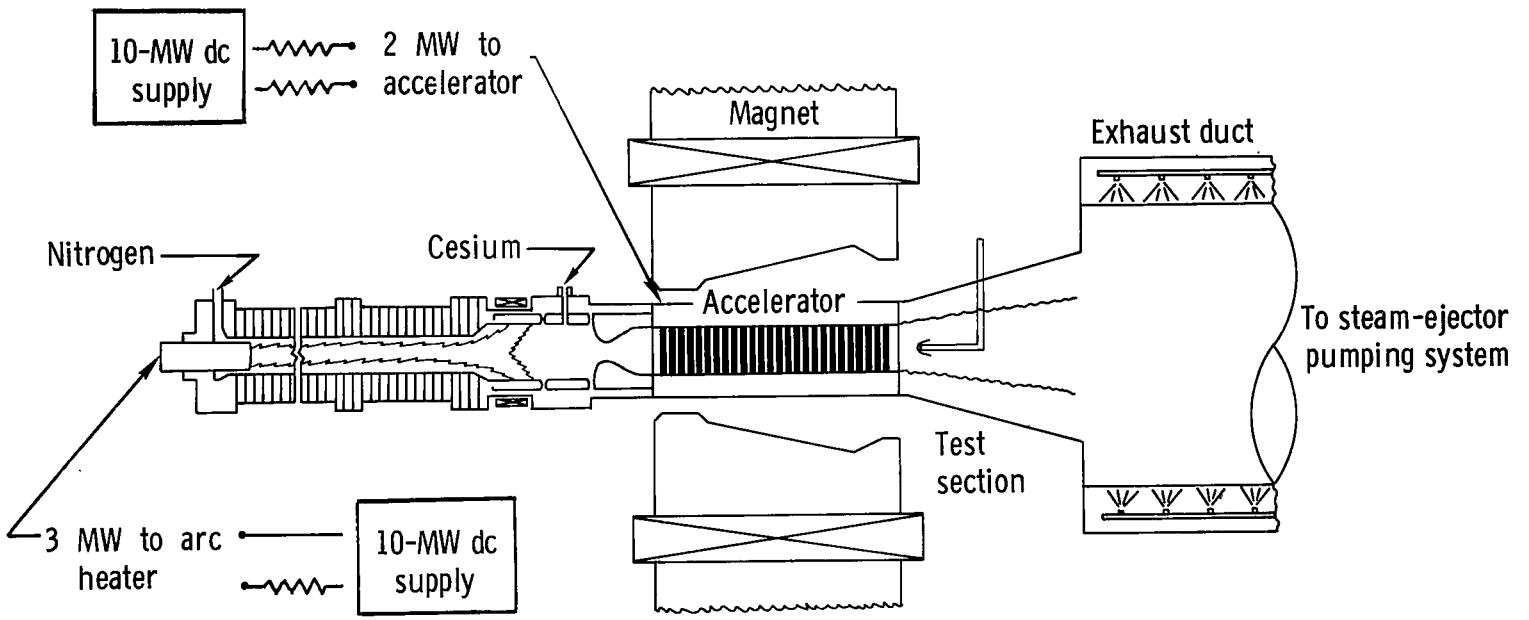

Figure 1.- Schematic diagram of the 20-megawatt linear plasma accelerator facility at the Langley Research Center.

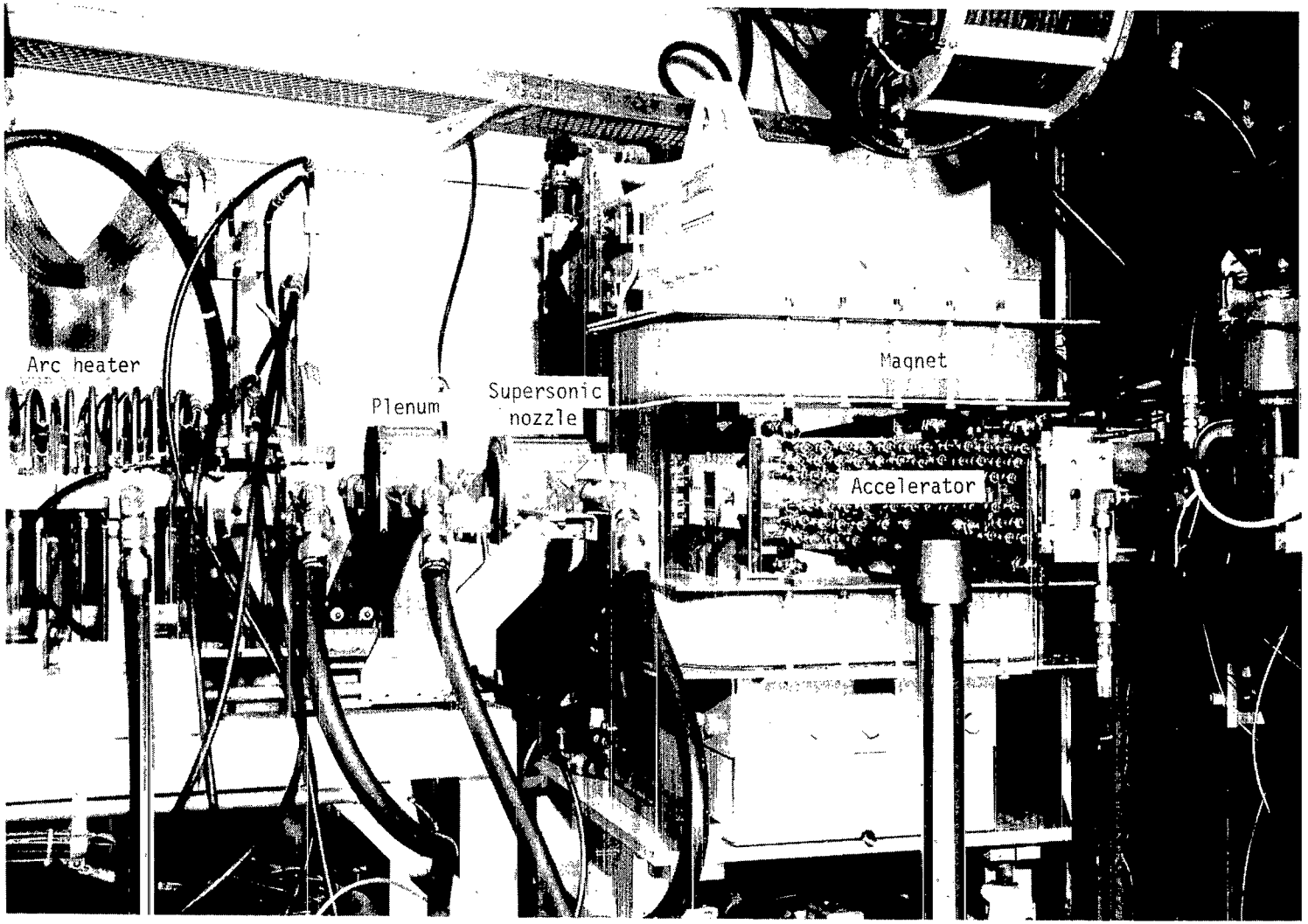

L-70-1255.1

Figure 2.- Arc heater, plenum, supersonic nozzle, magnet, and accelerator.

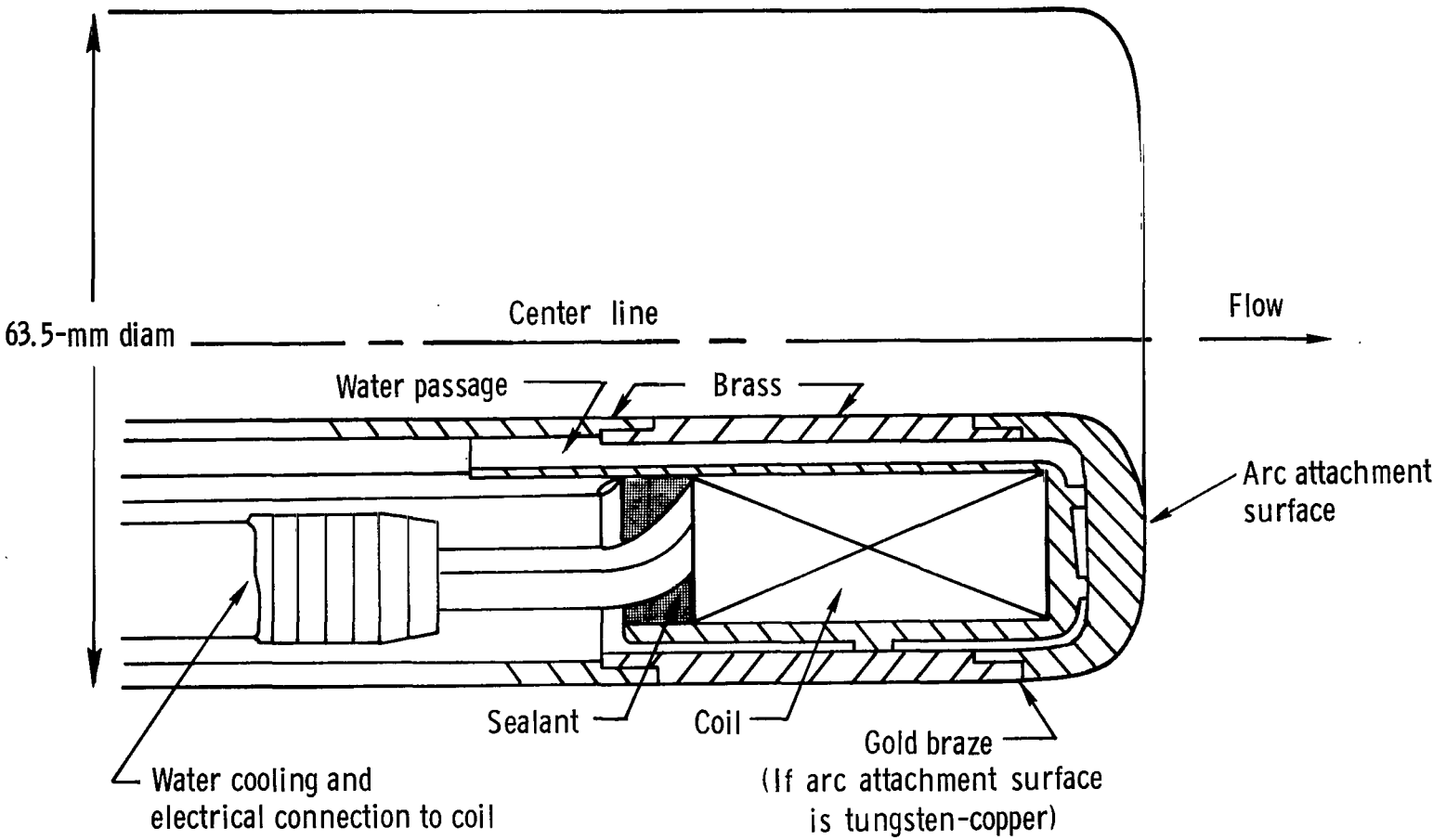

Figure 3.- Geometry of the original arc-heater cathode.

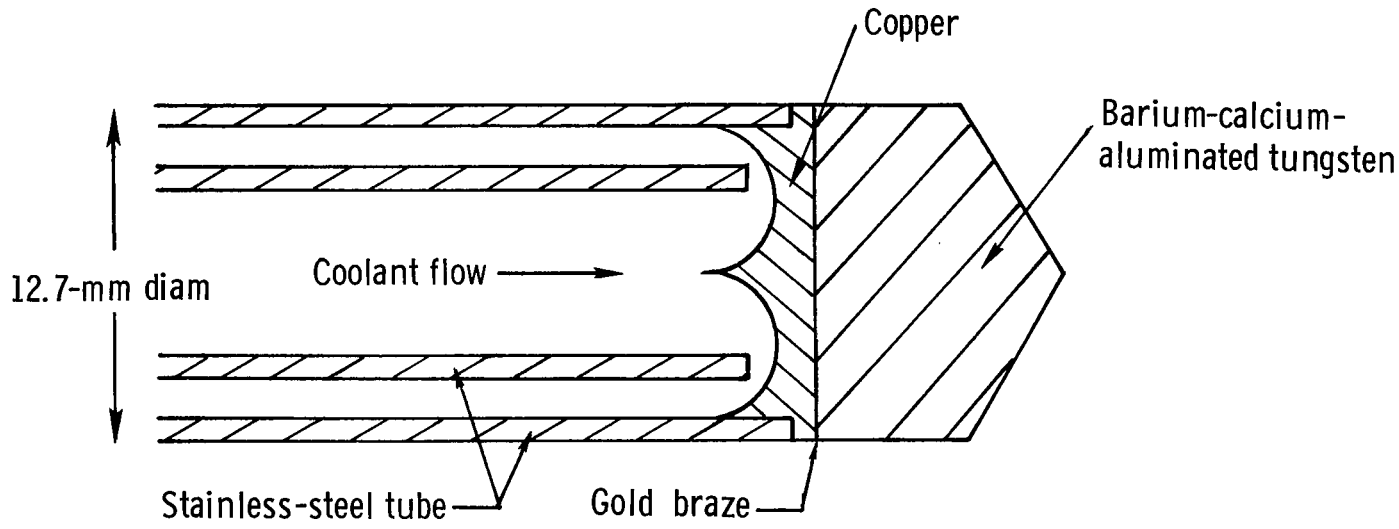

Figure 4.- A single element of the multiple cathode.

L-70-6915

Figure 5.- Cathode elements grouped in an axial configuration.
(Intermediate stage of development.)

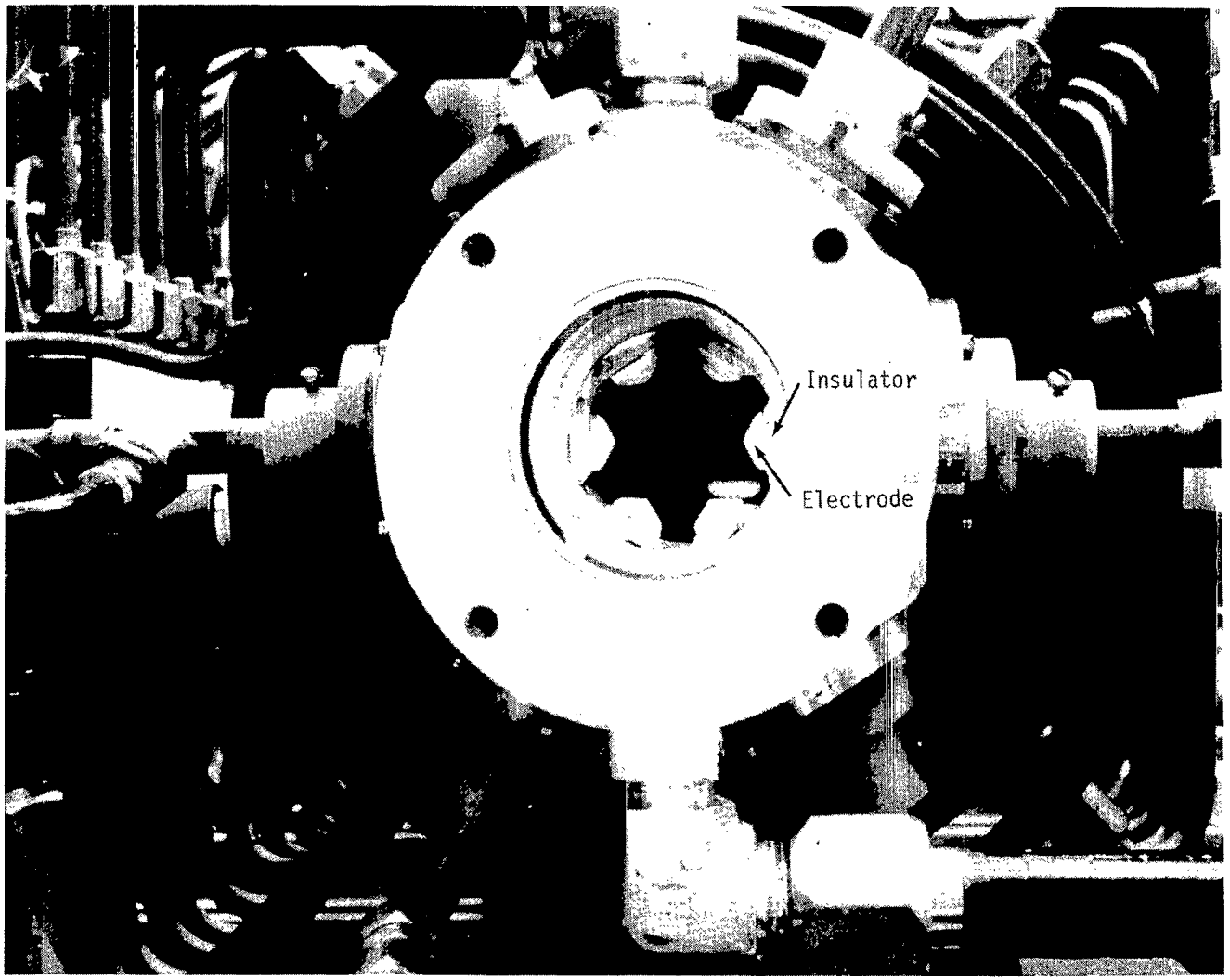

L-71-7116

Figure 6.- Cathode elements grouped in a radial configuration. View is along flow center line. (Final stage of development.)

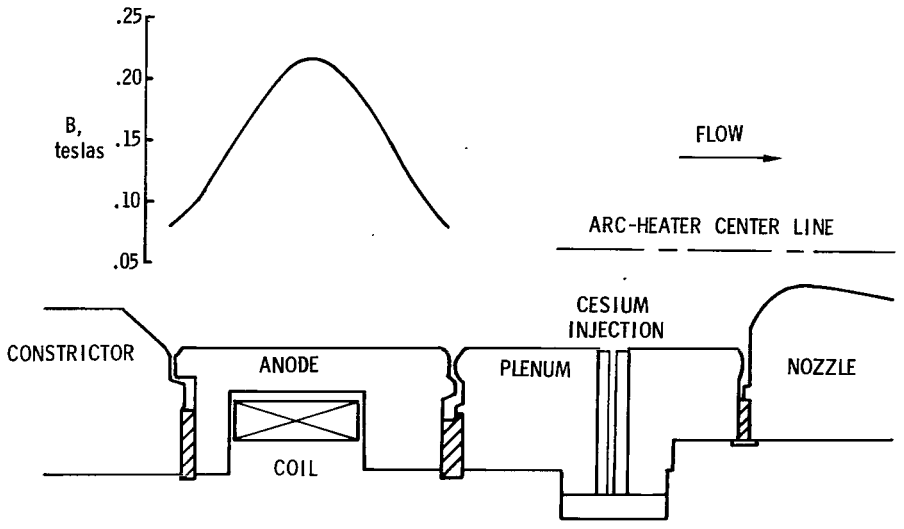

Figure 7.- Distribution of the axial magnetic-flux density at the anode wall with the original coil.

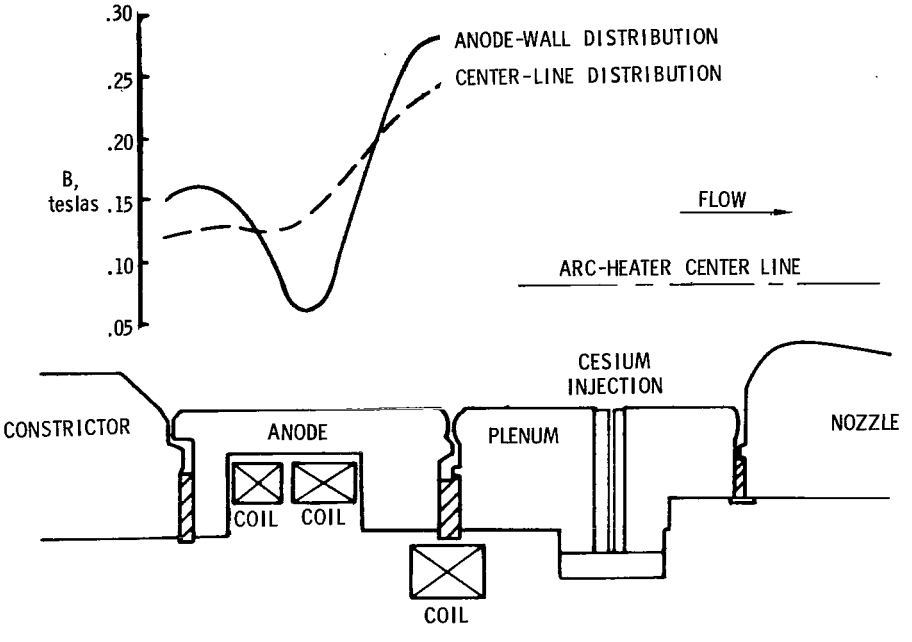

Figure 8.- Distribution of the axial magnetic-flux density at the anode wall and at the flow center line with the new coils.

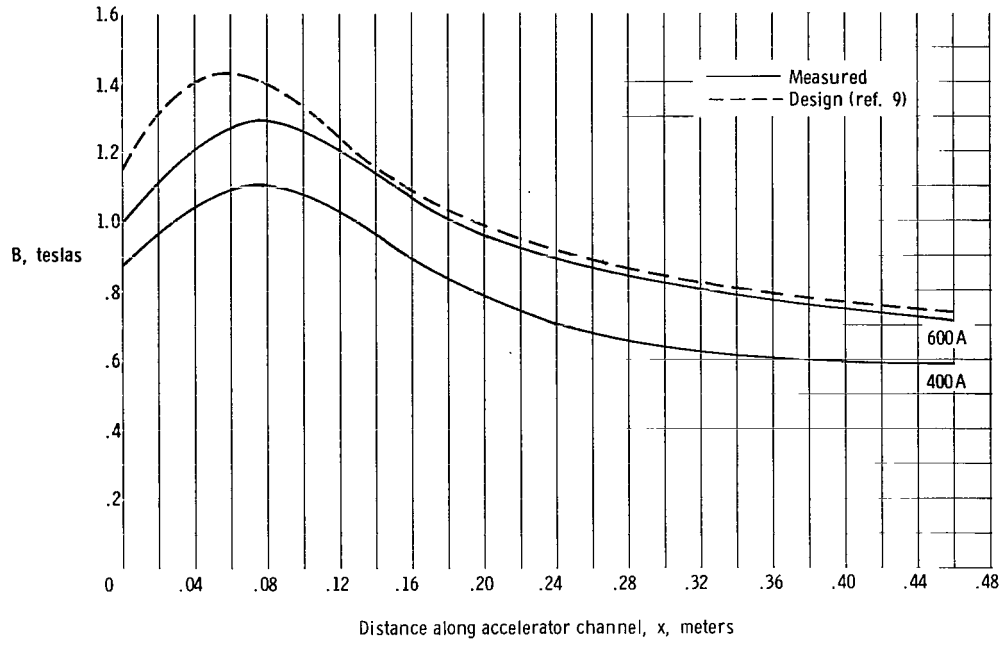

Figure 9.- Distributions of the original design and the measured magnetic-flux density.

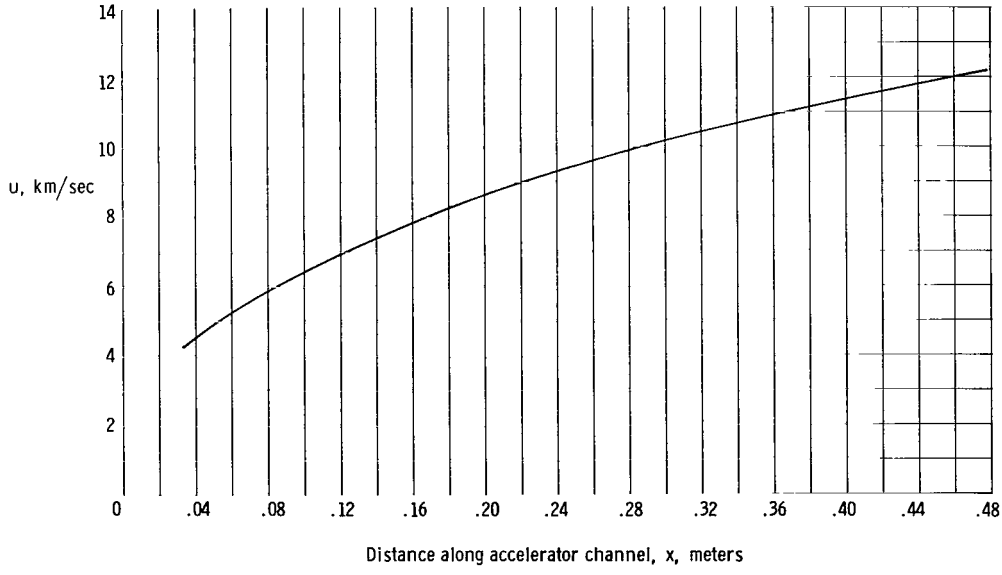

Figure 10.- Computed distribution of velocity for modified arc-heater conditions and measured magnetic-flux density.

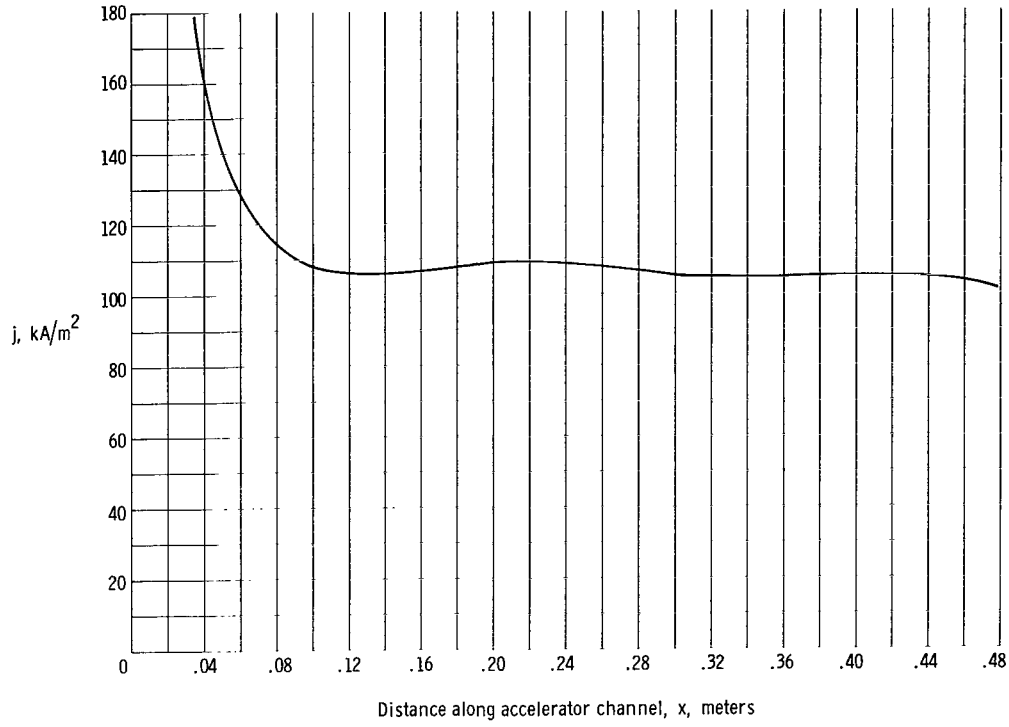

Figure 11.- Computed distribution of current density for modified arc-heater conditions and measured magnetic-flux density.

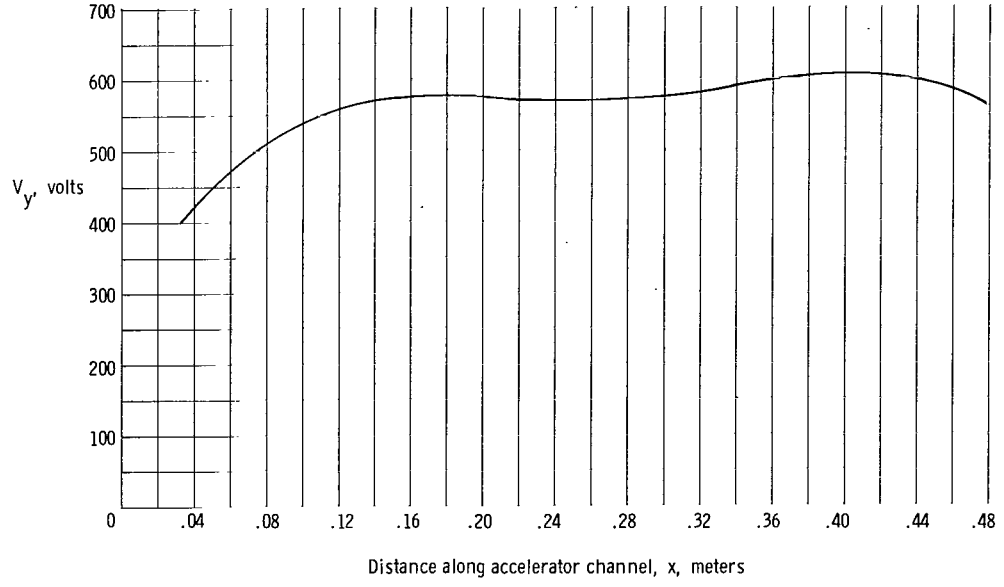

Figure 12.- Computed distribution of electrode potential difference across the channel for modified arc-heater conditions and measured magnetic-flux density.

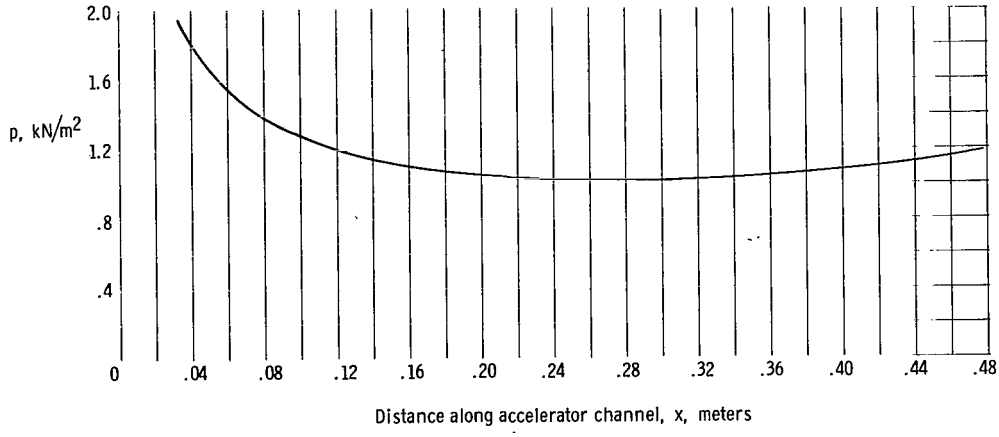

Figure 13.- Computed distribution of static pressure for modified arc-heater conditions and measured magnetic-flux density.

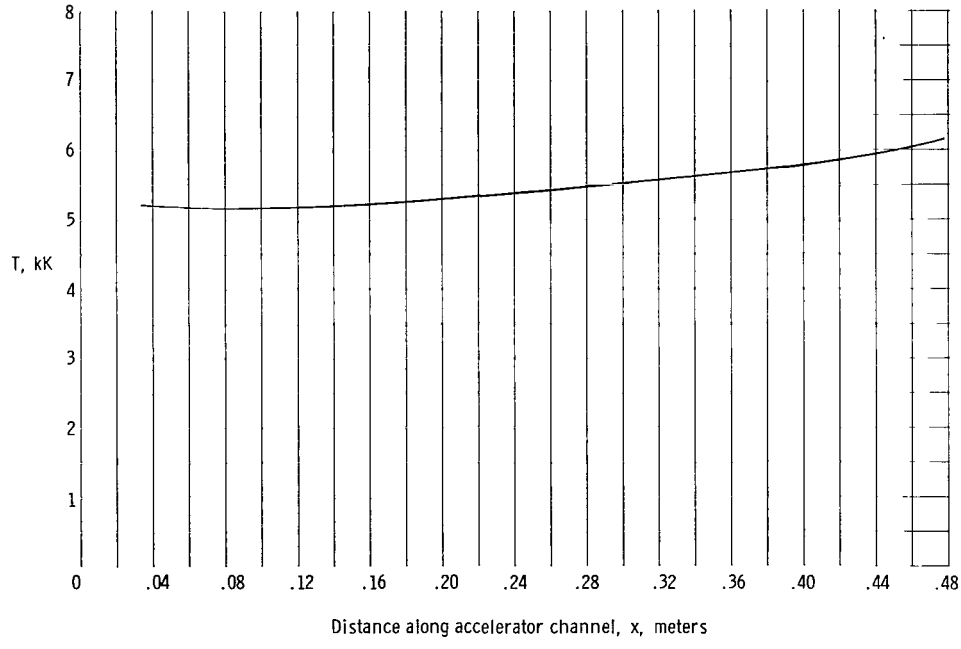

Figure 14.- Computed distribution of static temperature for modified arc-heater conditions and measured magnetic-flux density.

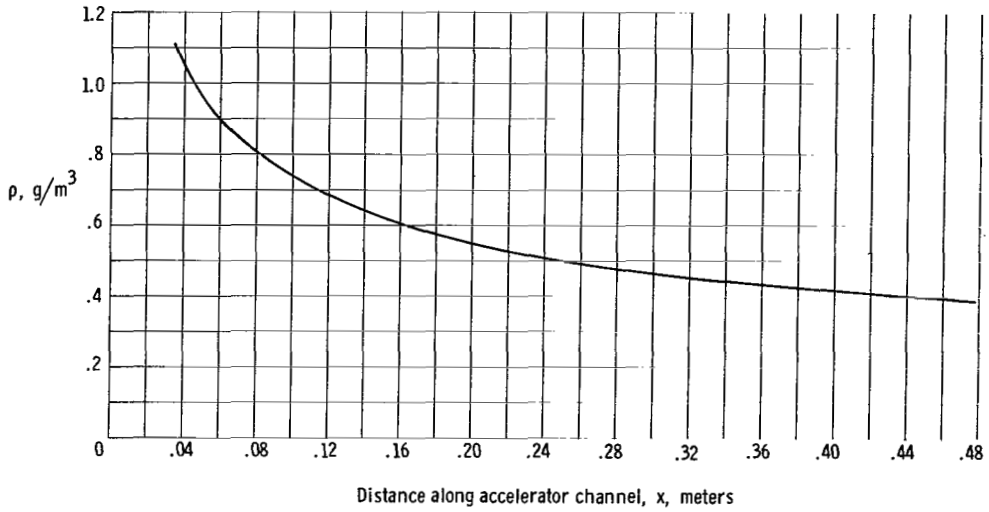

Figure 15.- Computed distribution of mass density for modified arc-heater conditions and measured magnetic-flux density.

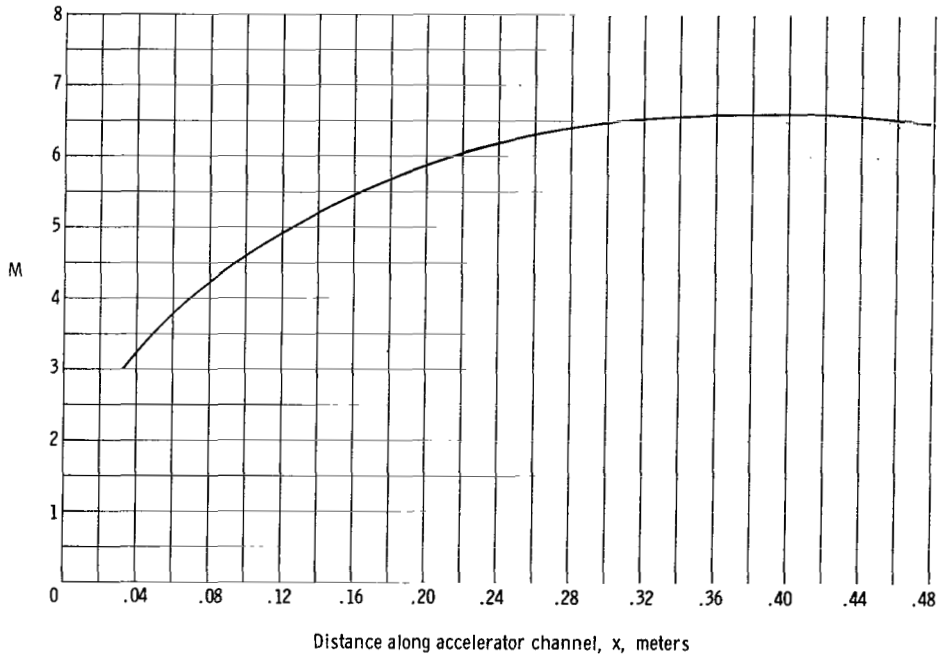

Figure 16.- Computed distribution of Mach number for modified arc-heater conditions and measured magnetic-flux density.

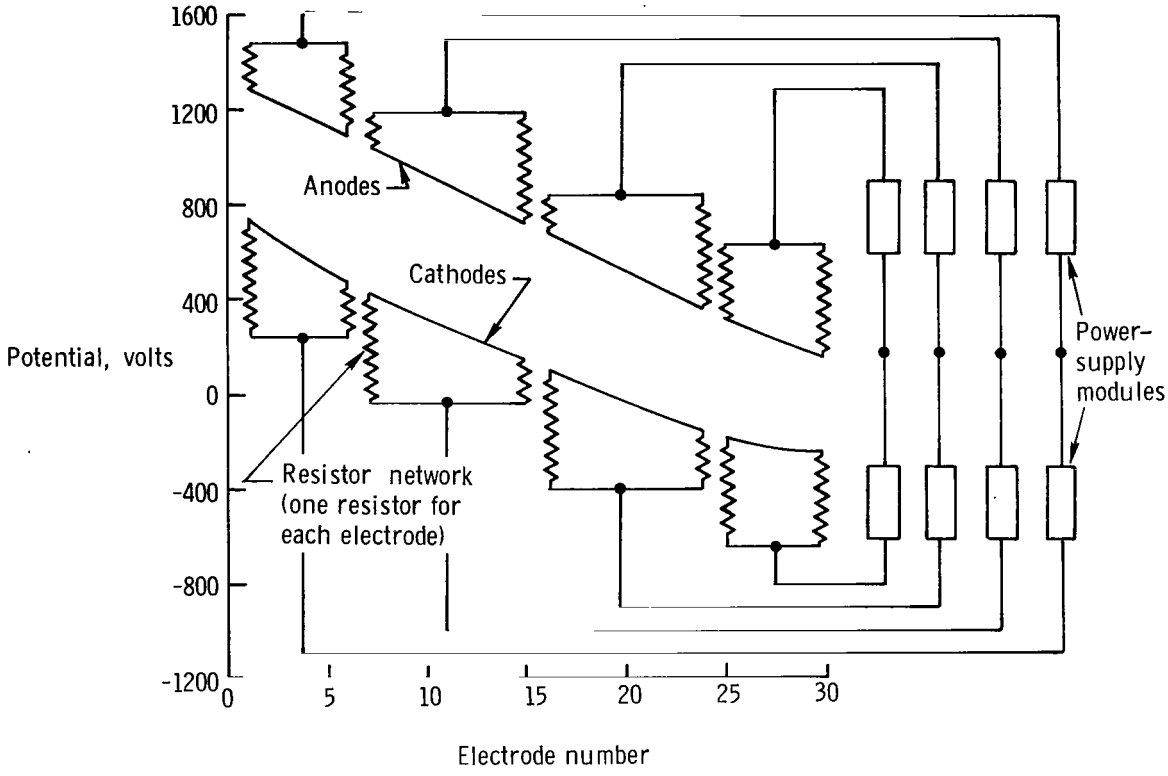

Figure 17.- Anode- and cathode-wall potential distributions, resistor network, and connections to power supply.

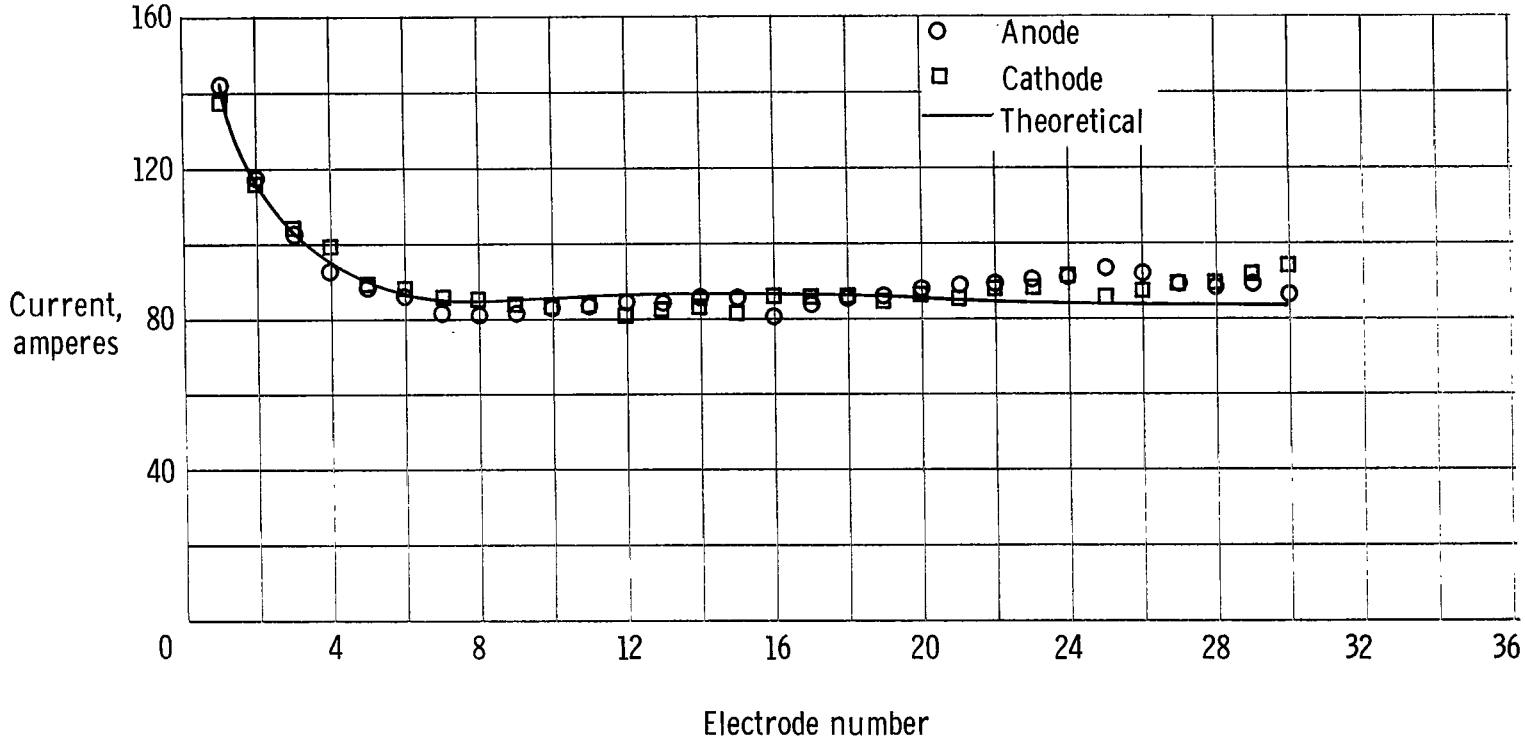

Figure 18.- Distributions of the computed and the measured accelerator electrode current.

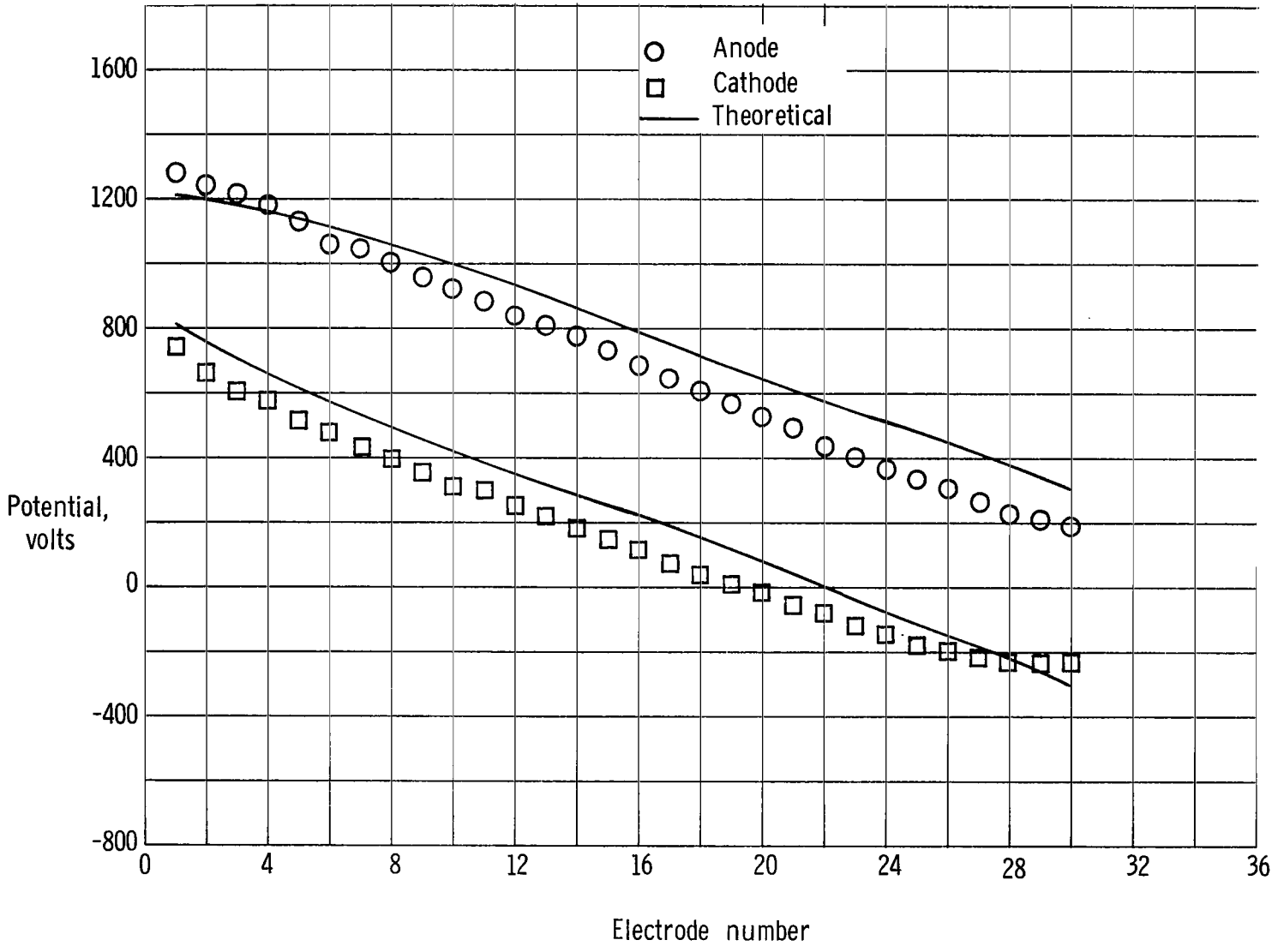

Figure 19.- Distributions of the computed and the measured anode-wall and cathode-wall potentials.

L-71-7117

Figure 20.- Bow shock wave on pitot tube at accelerator exit viewed perpendicular to the flow and probe center lines, which are coincident.

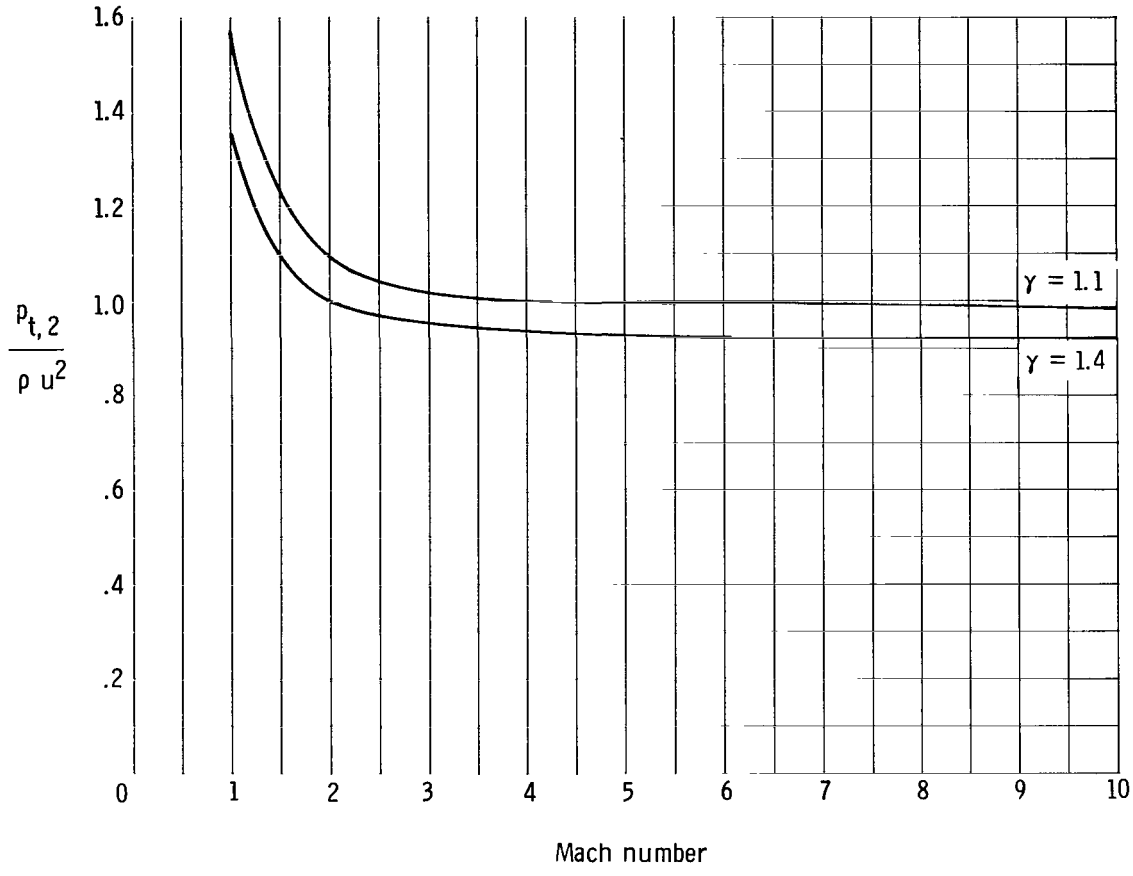

Figure 21.- The ratio of pitot pressure to ρu^2 as a function of the ratio of specific heats γ and Mach number.

NASA-Langley, 1971 —— 25 L-7932

019 001 C1 U 25 711210 S00903DS
DEPT OF THE AIR FORCE
AF WEAPONS LAB (AFSC)
TECH LIBRARY/WLOL/
ATTN: E LOU BOWMAN, CHIEF
KIRTLAND AFB NM 87117

"The aeronautical and space activities of the United States shall be conducted so as to contribute . . . to the expansion of human knowledge of phenomena in the atmosphere and space. The Administration shall provide for the widest practicable and appropriate dissemination of information concerning its activities and the results thereof."

—NATIONAL AERONAUTICS AND SPACE ACT OF 1958

NASA SCIENTIFIC AND TECHNICAL PUBLICATIONS

TECHNICAL REPORTS: Scientific and technical information considered important, complete, and a lasting contribution to existing knowledge.

TECHNICAL NOTES: Information less broad in scope but nevertheless of importance as a contribution to existing knowledge.

TECHNICAL MEMORANDUMS: Information receiving limited distribution because of preliminary data, security classification, or other reasons.

CONTRACTOR REPORTS: Scientific and technical information generated under a NASA contract or grant and considered an important contribution to existing knowledge.

TECHNICAL TRANSLATIONS: Information published in a foreign language considered to merit NASA distribution in English.

SPECIAL PUBLICATIONS: Information derived from or of value to NASA activities. Publications include conference proceedings, monographs, data compilations, handbooks, sourcebooks, and special bibliographies.

TECHNOLOGY UTILIZATION PUBLICATIONS: Information on technology used by NASA that may be of particular interest in commercial and other non-aerospace applications. Publications include Tech Briefs, Technology Utilization Reports and Technology Surveys.

Details on the availability of these publications may be obtained from:

SCIENTIFIC AND TECHNICAL INFORMATION OFFICE

NATIONAL AERONAUTICS AND SPACE ADMINISTRATION

Washington, D.C. 20546